Simultaneous Enhancement of Photothermal Stability and Gene Delivery Efficacy of Gold Nanorods Using Polyelectrolytes

Huang-Chiao Huang,[†] Sutapa Barua,[†] David B. Kay,[‡] and Kaushal Rege[†,§,*]

[†]Chemical Engineering, [‡]Bioengineering, and [§]Biological Design Program, Arizona State University, Tempe, Arizona 85287-6106

ABSTRACT The propensity of nanoparticles to aggregate in aqueous media hinders their effective use in biomedical applications. Gold nanorods (GNRs) have been investigated as therapeutics, imaging agents, and diagnostics. We report that chemically generated gold nanorods rapidly aggregate in biologically relevant media. Depositing polyelectrolyte multilayers on gold nanorods enhanced the stability of these nanoparticles for at least up to 4 weeks. Dispersions of polyelectrolyte (PE)-gold nanorod assemblies (PE—GNRs) demonstrate a stable Arrhenius-like photothermal response, which was exploited for the hyperthermic ablation of prostate cancer cells *in vitro*. Subtoxic concentrations of PE—GNR assemblies were also employed for delivering exogenous plasmid DNA to prostate cancer cells. PE—GNRs based on a cationic polyelectrolyte recently synthesized in our laboratory demonstrated higher transfection efficacy and lower cytotoxicity compared to those based on polyethyleneimine, a current standard for polymer-mediated gene delivery. Our results indicate that judicious engineering of biocompatible polyelectrolytes leads to multifunctional gold nanorod-based assemblies that combine high stability and low cytotoxicity with photothermal ablation, gene delivery, and optical imaging capabilities on a single platform.

KEYWORDS: gold nanorods · stability · photothermal · near-infrared · polyelectrolytes · cationic polymers · nonviral gene delivery · hyperthermia

Nanoparticles are being increasingly investigated as potential therapeutics, drug delivery vehicles, imaging agents, and diagnostics as part of the expanding field of nanomedicine.[1−5] The unique plasmonic properties of gold nanoparticles make them attractive candidates in a number of biological applications including drug delivery and imaging. In particular, gold nanorods demonstrate a tunable photothermal response to near-infrared (NIR) light as a function of nanoparticle aspect ratio.[6,7] While the transverse absorption of gold nanorods is at a wavelength of 520 nm, the longitudinal peak can be tuned to different regions of the absorption spectrum as a function of the nanorod length. Consequently, gold nanorods have been employed in diagnostics,[8,9] therapeutic systems,[10−13] imaging,[14] sensing,[15−17] and responsive materials/assemblies.[18,19]

The photothermal response of gold nanoparticles, including nanorods, nanoshells, and nanocages, has been exploited for the hyperthermic destruction of cancer cells.[20,21] The ability to generate high temperatures at a desired site with externally tunable control holds significant promise for cancer therapy over whole-body hyperthermia. In this approach, gold nanorods can be targeted to the tumor *in vivo* and subjected to laser irradiation from an external source, leading to the selective localization of hyperthermic treatment.[22] Both, targeted and nontargeted methods (*e.g.*, using targeting antibodies or aptamers) can be exploited for the photothermal ablation of cancer cells using gold nanorods. In addition to hyperthermic ablation of cancer cells, gold nanoparticles have also been investigated for delivering drugs[23−28] and exogenous nucleic acids[29−34] to cells. Properties such as biocompatibility, ease of functionalization, and near-infrared imaging make gold nanorods promising as theranostic platforms.

A variety of techniques, including those based on chemical[35] and electrochemical[36,37] methods, have been employed for the generation of gold nanorods. In particular, cetyltrimethyl ammonium bromide (CTAB)-templated growth is a popular method for making gold nanorods (GNRs) in aqueous dispersion media.[35] GNRs with peak longitudinal wavelengths in the visual and near-infrared region of the absorption spectrum can be reproducibly synthesized using this method. CTAB forms a bilayer on the surface of the nanorods and repulsion between the cationic quaternary ammonium head groups of the surfactant results in stable

*Address correspondence to Kaushal.Rege@asu.edu.

Received for review March 18, 2009 and accepted August 27, 2009.

Published online September 16, 2009.
10.1021/nn900947a CCC: $40.75

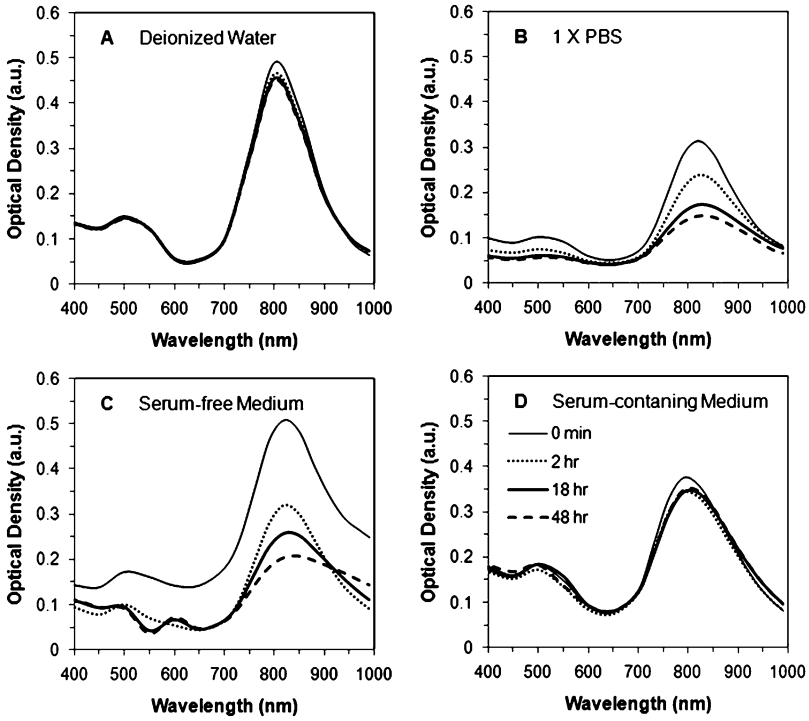

Figure 1. Short-term optical stability of CTAB−gold nanorods (CTAB−GNRs) dispersed in different biologically relevant media. CTAB−GNRs, optical density 0.5 at 800 nm, were centrifuged once and resuspended in same volume of (A) deionized or DI water, (B), phosphate-buffered saline (PBS) (C) serum-free medium, and (D) serum-containing medium. Absorbance spectra were monitored from 400 to 999 nm for up to 48 h in respective media.

gold nanorod dispersions in certain aqueous media. However, different modification strategies,[38−44] have been investigated for replacing CTAB on nanorods in order to adapt gold nanorods for diverse biological applications and in order to overcome CTAB toxicity.[38,45]

We report that short-term and long-term stability of gold nanorods depends on the media in which these nanoparticles are dispersed. As-prepared gold nanorods, centrifuged only once in order to remove CTAB present in the dispersion, are not stable in phosphate-buffered saline (PBS) and serum-free media (SFM), while they are stable in deionized (DI) water and serum-containing media (SCM). However, gold nanorods are stable only in DI water following an additional two rounds of centrifugation (total three centrifugation steps) carried out to remove excess CTAB. We investigated the use of layer-by-layer polyelectrolyte deposition on nanoparticle surfaces[46] as means to enhance gold nanorod stability. Optical stability, determined using absorbance in the near-infrared (NIR) region of the absorption spectrum, and thermal stability, determined using the dispersion temperature response following laser irradiation of gold nanorods, were maintained for at least 4 weeks following nanorod coating with alternating layers of anionic and cationic polyelectrolytes (polyelectrolyte−coated-gold nanorods or PE−GNRs). PE−GNRs demonstrated a stable and tunable photothermal response which was exploited for the ablation of prostate cancer cells. In addition, PE−GNRs were employed to successfully transfect PC3-PSMA prostate cancer cells with plasmid DNA, in contrast to CTAB−GNRs which did not demonstrate any transfection efficacy. GNRs coated with a recently synthesized polymer from our laboratory demonstrated significantly lower cellular toxicities than poly(ethyleneimine), the current standard for polymeric gene delivery.

RESULTS AND DISCUSSION

Polyelectrolytes Enhance Short-Term and Long-Term Stability of Gold Nanorods Dispersed in Biologically Relevant Media. A facile method for preparing gold nanorods involves the use of cetyltrimethyl ammonium bromide (CTAB) as a template for nanorod growth.[35] We first investigated the short-term stability of as-prepared CTAB gold nanorods (CTAB−GNRs) in different aqueous media including deionized (DI) water, phosphate-buffered saline (PBS), serum-free media (RPMI-1640), and serum-containing media (RPMI-1640 + 10% fetal bovine serum or FBS). The nanorods were centrifuged once as part of the synthesis protocol in order to remove excess CTAB in the aqueous dispersion and resuspended in equivalent volumes of the respective media. The short-term optical stability was determined by following the longitudinal peak in the near-infrared region of the absorbance spectrum as a function of time for 48 h. As seen in Figure 1A, gold nanorods formed stable dispersions in DI water; the longitudinal peak was maintained over the period of the investigation (48 h). However, the absorbance of CTAB−GNRs decreased rapidly in PBS (Figure 1B) and serum-free media (SFM; Figure 1C). The peak absorbance values were found to be approximately 60−70% of the initial values following only 2 h of dispersion in the two media, indicating rapid aggregation of the nanorods in PBS and SFM. The aggregation is induced presumably because of the higher salt concentration (~150 mM) of these solutions, which screened repulsive interactions between individual CTAB-covered nanorods. However, CTAB−GNRs demonstrated excellent stability in serum-containing media (SCM; Figure 1D) with no loss in absorbance in the NIR peak over 48 h. It is possible that interactions with serum proteins (*e.g.*, albumin) resulted in enhanced stability of gold nanorods[47,48] in serum-containing media.

It has been reported that multiple centrifugation rounds are necessary to remove excess CTAB from gold nanorod dispersions.[49] However, centrifugation can also result in the loss of CTAB molecules self-assembled on the surface of the gold nanorods resulting in their aggregation. We investigated the role of subsequent centrifugation rounds on the stability of CTAB−GNRs in aqueous

media. In this case, we monitored both short- (up to two days; not shown) and long-term (up to 4 weeks; Figure 2) stability of CTAB−GNRs following two additional rounds of centrifugation. While CTAB−GNRs were stable in DI water, they aggregated in PBS, SFM, and SCM after three rounds of centrifugation, leading to a complete loss of their light absorption properties in the near-infrared region (Figure 2). While the stability of CTAB−GNRs is excellent in DI water, their poor stability in biological media can limit their utility in biological applications.

Various strategies have been investigated for enhancing the stability of nanoparticles in aqueous media. For example, self-assembly/conjugation with polyethylene glycol (PEGylation) is an attractive method for enhancing nanoparticle stability.[50] However, the presence of PEG on nanoparticle surface results in reduced interactions with proteins and uptake by cells.[50] While this is desirable in some cases, it might not be desirable in cases where the nanorods might be employed for applications such as gene delivery which require cellular binding and uptake. We have recently generated a novel library of cationic polyelectrolytes for enhancing binding to anionic plasmid DNA leading to efficient transfection of mammalian cells.[51] We asked whether coating CTAB−GNRs with polyelectrolyte layers could result in stable dispersions of gold nanorods that also demonstrate high gene delivery and photothermal ablation efficacies.

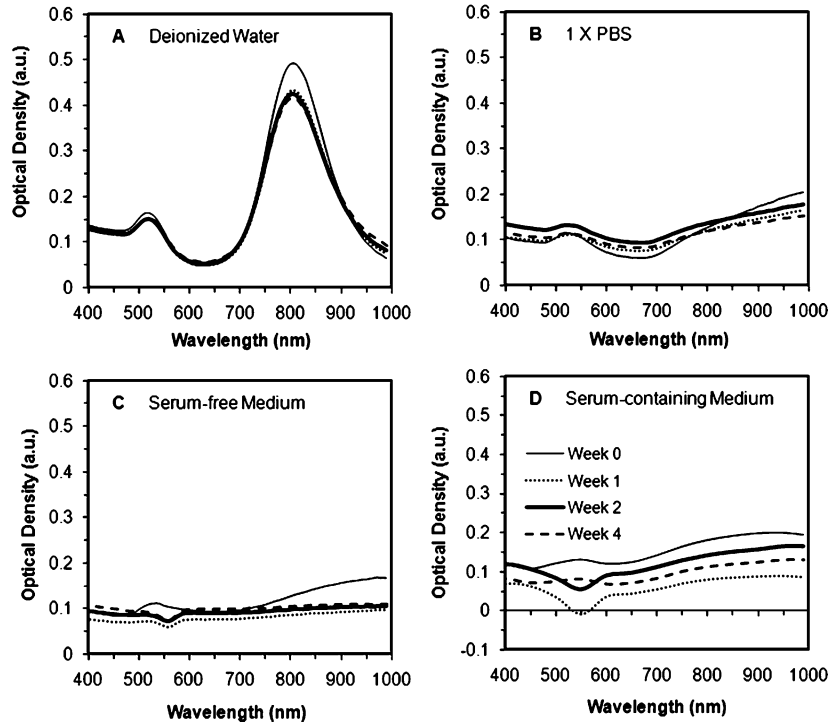

Figure 2. Long-term UV−visible spectra of CTAB−GNRs dispersed in different biologically relevant media. CTAB−GNRs, optical density 0.5 at 800 nm were centrifuged three times and resuspended in same volume of (A) deionized water, (B) PBS, and (C) serum-free medium, and (D) serum-containing medium. Spectra were measured immediately following preparation ("week 0"), 1, 2, and 4 weeks after preparation. Similar results were seen with GNRs with a maximal absorption peak at 750 nm.

Following centrifugation, CTAB−GNRs were first coated with the anionic polymer poly(styrene sulfonate) (PSS). The resulting PSS−CTAB−GNRs were centrifuged once in order to remove excess PSS and the supernatant was decanted. The PSS−CTAB−GNRs were then resuspended in solutions containing different concentrations of the cationic polymers pEI25 or EGDE-3,3′ in 0.01 X PBS (PBS diluted 100 fold; pH = 7.4, salt concentration 1.5 mM) leading to the formation of pEI25−PSS−CTAB−GNRs or EGDE-3,3′−PSS−CTAB−GNRs. The EGDE-3,3′ cationic polyelectrolyte was generated using the ring-opening polymerization of ethyleneglycol diglycidylether and 3,3′-diamino-*N*-methyl dipropylamine as described previously.[51] Following equilibration with PSS−CTAB−GNRs, excess cationic polymer was removed by centrifugation and the polyelectrolyte-nanorod assemblies were dispersed in serum-free medium in order to investigate their optical stability. As seen in Figure 3i, low concentrations of the EGDE-3,3′ polymer did not enhance the stability of the gold nanorods, which aggregated presumably due to bridging between the PSS layer and EGDE-3,3′ polymer layer between different nanorods. Aggregation of GNRs led to a loss of the longitudinal peak in the NIR region. However, "recovery" of the NIR peak was made possible by increasing the concentration of the EGDE-3,3′ polymer (Figure 3iC,D). Increasing EGDE-3,3′ polymer adsorption on PSS−CTAB−GNRs leads to interparticle repulsion due to an increase in cationic charges on the surface, and therefore, results in enhanced stability of the gold nanorod dispersion. As seen in Figure 3iD, the short-term stability of these dispersions was significantly enhanced compared to CTAB−GNRs.

In addition to the EGDE-3,3′ polymer, we investigated the efficacy of another cationic polymer, 25 kDa polyethyleneimine (pEI25), for stabilizing GNRs. As seen in Figure 3iiA−D, pEI25 showed similar trends to EGDE-3,3′-coated nanorods. Low concentrations of pEI25 resulted in aggregation and loss of the NIR absorption peak due to bridging with the anionic PSS layers. However, pEI25-PSS−CTAB−GNRs formed stable dispersions in the media with an increase in pEI25 concentration. The amount of cationic polyelectrolyte required for NIR peak recovery was similar in cases of both, the EGDE-3,3′ polymer and pEI25; gold nanorods stabilized with 3 mg/ml cationic polyelectrolytes were used in subsequent experimentation.

While the short-term stability results with PE−GNR assemblies were indeed promising, we investigated whether the use of polyelectrolytes could keep the nanorod dispersions stable over a longer period of time. The

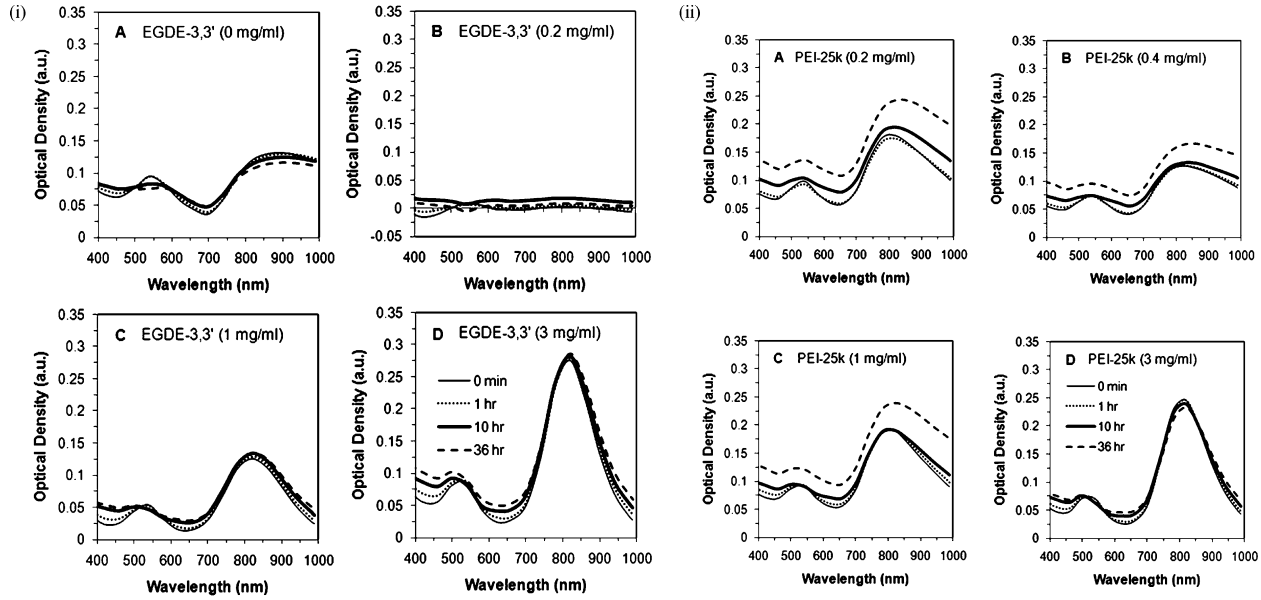

Figure 3. Stability of (i) EGDE-3,3′—PSS—CTAB—GNRs, (ii) pEI25-PSS—CTAB—GNRs in serum free media as monitored by the transverse and longitudinal absorption peaks. CTAB nanorods were coated with the anionic polyelectrolyte PSS (2 mg/mL), followed by coating with different concentrations of cationic polyelectrolytes, (i) EGDE-3,3′ and (ii) pEI25. In panel set i: (A) 0 mg/mL, (B) 0.2 mg/mL, (C) 1 mg/mL, and (D) 3 mg/mL EGDE-3,3′ polymer. In panel set ii, (A) 0.2 mg/mL, (B) 0.4 mg/mL, (C) 1 mg/mL, and (D) 3 mg/mL, pEI-25k polymer. The absorption spectra of polyelectrolyte-coated GNRs were monitored for up to 36 h using a temperature-controlled plate reader (see Experimental Section for details).

absorption properties of EGDE-3,3′ and pEI25-based gold nanorods remained invariant over a period of 4 weeks in serum-free media (Figure 4 A,B). The near-infrared (NIR) absorption peak (~770 nm) was maximal following immediate preparation of the nanorods (0 day) in serum-containing media. However, the peak absorbance value settled to a lower maximum in 1 week and was found to be stable thereafter. It is possible that serum-polyelectrolyte interactions result in the precipitation of a portion of the nanorods dispersed in serum-containing media over the period of one week, leading to a reduction in the NIR peak absorbance. Taken together, polyelectrolytes stabilize gold nanorod dispersions in both serum-free and serum-containing media over extended periods of time, making this a viable strategy for their use in biological applications.

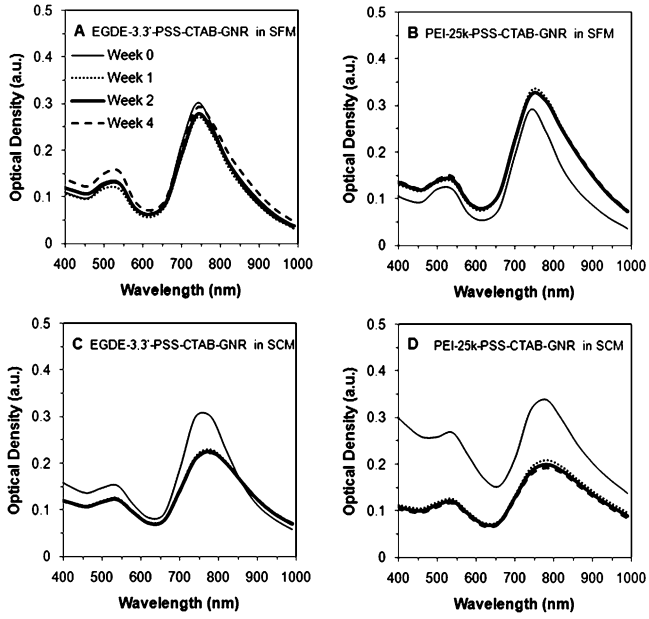

Figure 4. Long-term UV—visible spectra of polyelectrolyte-coated gold nanorods (PE—GNRs) dispersed in serum-free media and serum-containing media. EGDE-3.3′—PSS—CTAB—GNRs (λ_{max} = 770 nm) dispersed in serum-free media (A) and serum-containing media (C); pEI25k—PSS—CTAB—GNRs dispersed in serum-free media (B) and serum-containing media (D).

EGDE-3,3′—PSS—CTAB—GNRs Demonstrate Lower Cytotoxicities Than pEI25-PSS—CTAB—GNRs. We evaluated the cytotoxicity of pEI25-PSS—CTAB—GNRs toward PC3-PSMA human prostate cancer cells and compared it to that of EGDE-3,3′—PSS—CTAB—GNRs. Following treatment with different PE—GNR concentrations, cells were treated with ethidium homodimer which fluoresces red in dead/dying cells. Figure 5ii,iii show the phase contrast and fluorescence microscopy images of cells treated with different concentrations of the PE—GNRs shown in Figure 5i. As seen in Figure 5ii—iv, EGDE-3,3′-coated GNRs were less toxic to cells than pEI25-coated GNRs indicating that the candidate from a recently generated polymer library in our laboratory[51] demonstrated less cytotoxicity than pEI25, which is a standard for polymer-mediated gene delivery. However, we found that EGDE-3,3′-coated GNRs were more toxic than as-prepared CTAB—GNRs (centrifuged once) at comparable optical densities (not shown). It is not clear whether the aggregation of CTAB—GNRs reduces the interaction of surface CTAB molecules with cells leading to lower toxicities. In addition, CTAB—GNR aggregation can also result in reduced uptake due to increased size, and therefore lower toxicities toward cells.

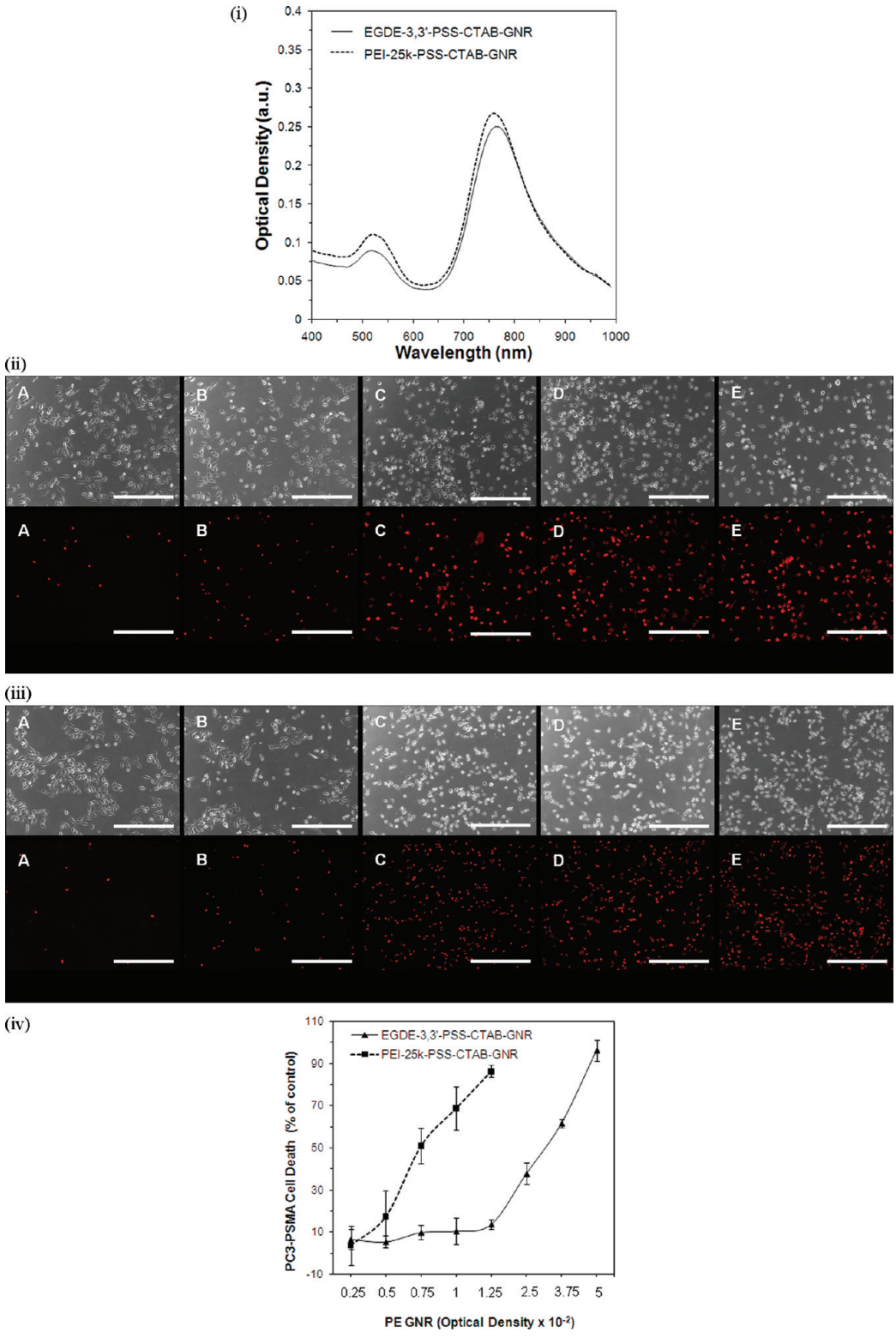

Figure 5. Cytotoxicity of polyelectrolyte-coated gold nanorods (PE−GNRs): (i) Absorption spectra of PE-coated nanorods employed in the cytotoxicity analysis; (ii) phase contrast and fluorescence microscopy images that show the cytotoxicity of EGDE-3,3′−PSS−GNRs, toward PC3-PSMA cells. Red fluorescent ethidium homodimer, which stains DNA in compromised nuclei, was used to determine cytotoxicity following 6 h treatment. A total of 10, 25, 50, 75, and 100 μL of EGDE-3,3′-PSS−CTAB−GNRs (optical density (OD) = 0.25), was added to cells. The final volume in each well was brought up to 500 μL, resulting in final optical densities of (A) 0.005; (B) 0.0125; (C) 0.025, (D) 0.0375, and (E) 0.05. Scale bar: 500 μm. (iii) Phase contrast and fluorescence microscopy images that show the cytotoxicity of pEI25−PSS GNRs: (A) 5 μL (OD = 0.0025), (B) 10 μL (OD = 0.005), (C) 15 μL (OD = 0.0075), (D) 20 μL (OD = 0.01), and (E) 25 μL (OD = 0.0125) of pEI25−PSS−GNRs. Other conditions are similar to those described above. Scale bar: 500 μm. (iv) Comparison of cytotoxicity of pEI25−PSS−CTAB−GNRs and EGDE-3,3′−PSS−CTAB−GNRs as a function of PE−GNR optical density.

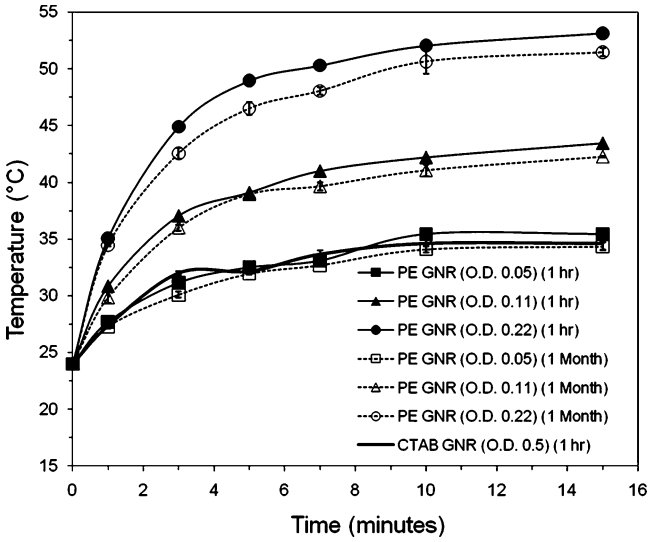

Figure 6. Photothermal response of EGDE-3,3′—PSS—CTAB—GNRs in serum-free media. Different concentrations (as determined by their optical densities) of nanorods were irradiated with continuous wavelength (CW) laser at 770 nm (20 W/cm^2) for a maximum of 15 minutes. The temperature of the dispersion was monitored using a K-thermocouple. The steady-state temperatures showed an increase of approximately 10 °C with a doubling of nanorod concentration indicating Arrhenius-like behavior.

Polyelectrolytes Maintain Long-Term Photothermal Activity of GNRs. Photothermal properties of gold nanorods have been employed in various biomedical applications including, ablation of cancer cells, sensors, and diagnostics. We investigated the photothermal response of polyelectrolyte-stabilized gold nanorods 1 h after preparation and after 4 weeks of storage in serum-free media in order to determine if these properties were also maintained over a period of time. As seen in Figure 6, PE-stabilized gold nanorods demonstrated a reproducible photothermal response as a function of the nanorod concentration in the dispersion. The temperature of the media rose rapidly in the first 5 minutes of laser exposure after which, the temperature either rose gradually as in the case of higher nanorod concentrations or remained invariant as in the case of lower nanorod concentrations. Interestingly, the steady-state temperature of the dispersion increased by approximately 10 °C following a doubling of the gold nanorod concentration (as determined by the nanorod optical density), indicating that the photothermal response of PE—GNR dispersion followed Arrhenius-like behavior. Importantly, the photothermal response of EGDE-3,3′-coated gold nanorods after 4 weeks of storage closely followed the same trend observed for freshly prepared nanorods for all concentrations employed in the investigation (Figure 6). However, CTAB—GNRs demonstrated a lower photothermal response compared to EGDE-3,3—PSS—CTAB—GNRs only 1 h after preparation; while the temperature increase with EGDE-3,3—PSS—CTAB—GNRS (OD = 0.22) was approximately 53 °C after 15 min of exposure to the laser, the temperature of a dispersion containing a higher concentration of CTAB—GNRs (*i.e.*, OD = 0.5) rose only to 32 °C after an equivalent laser exposure time. Expectedly, these results correlate well with optical stability in that gold nanorods that demonstrate stable optical behavior also demonstrate effective photothermal behavior. Conversely, aggregation leads to a loss in the photothermal efficacy of CTAB—GNRs. Taken together, polyelectrolyte-mediated stabilization helps maintain the optical as well as photothermal properties of gold nanorods for extended periods of time.

EGDE-3,3′—PSS—CTAB—GNRs Induce Photothermal Ablation of PC3-PSMA Human Prostate Cancer Cells. The ability of plasmonic gold nanostructures to convert near-infrared (NIR) radiation to heat energy has been exploited for inducing hyperthermic death of cancer cells. We therefore asked if EGDE-3,3′—PSS—CTAB—GNRs could induce death in PC3-PSMA human prostate cancer cells following NIR laser irradiation. Cells were treated with a final concentration of 0.1 OD of EGDE-3,3′—PSS—CTAB—GNRs (absorbance spectrum in Figure 7i) which resulted in a final temperature of approximately 42 °C following seven minutes of laser irradiation (Figure 6). Laser irradiation induced significant cell death in PC3-PSMA human prostate cancer cells after 24 h of PE—GNR treatments (Figure 7ii A,B). Although cell morphology remained invariant immediately after PE—GNR/laser treatment, extensive changes in cell morphology and high ethidium homodimer staining of compromised nuclei were seen after 24 h, indicating that cell death occurred presumably due to apoptosis of these cells. Negligible loss of cell viability was observed in PC3-PSMA cells treated with EGDE-3,3′—PSS—CTAB—GNRs but not exposed to NIR laser irradiation (Figure 7iiC,D), laser alone (Figure 7iiE,F); the viability of these cells was similar to untreated PC3-PSMA cells (Figure 7iiG,H).

PC3-PSMA cells were treated with EGDE-3,3′—PSS—CTAB—GNR assemblies (OD = 0.1) and subjected to different power densities ranging from 7.5—25 W/cm^2 in order to investigate if tuning laser power densities resulted in differential cell death. As seen in Figure 7iii, increasing laser power density resulted in an increase in media temperature in correlation with the extent of PC3-PSMA cell death. Interestingly, PC3-PSMA cell death was as high as 55% and 70%, following laser treatment at power densities 7.5 and 15 W/cm^2, even though the media temperature was only 30 and 35 °C, respectively. This apparent discrepancy can be explained due to two reasons. First, the temperature measurements were carried out immediately after the laser was turned off. It is possible that these recordings were somewhat lower than those during the photothermal treatment, especially in the case of cells directly in the path of the laser spot which was 2 mm in diameter (well diameter ~6.5 mm). Second, it is important to note that negligible cell death was seen immediately after the seven-minute laser treatment and that the cell vi-

(i)

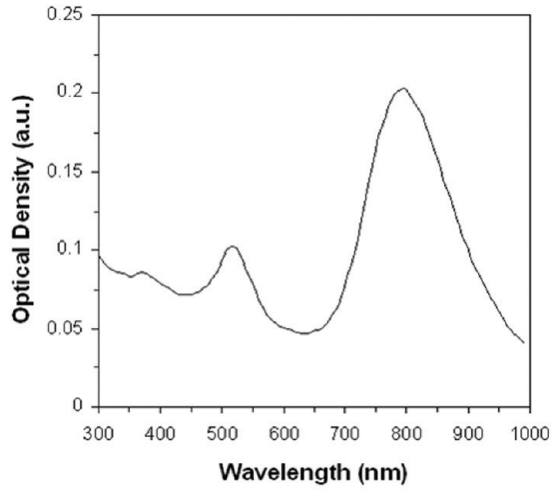
Optical Density (a.u.)
0.25
0.2
0.15
0.1
0.05
0
300
400
500
600
700
800
900
1000
Wavelength (nm)

(ii)

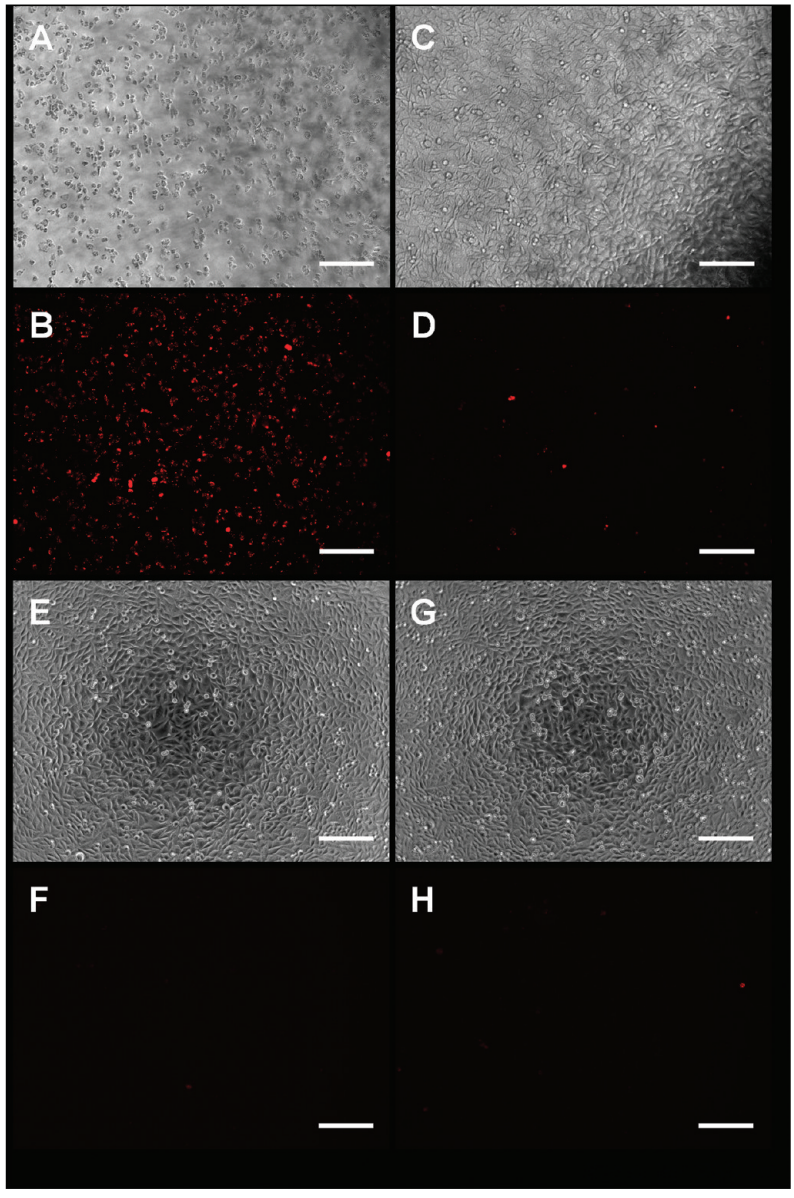
A
C
B
D
E
G
F
H

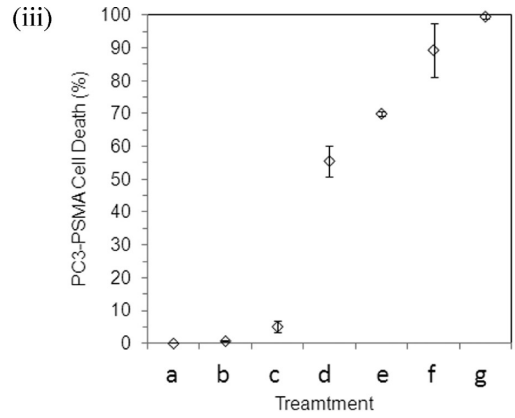

Treatments	Details	Media Temperature (°C)
a	Live Control: No treatment.	22±0.5
b	Laser Control: Laser 25 W/cm^2 for 7 minutes.	25±0.7
c	PE-GNR Control: Laser 0 W/cm^2 for 7 minutes.	22±0.5
d	Laser treatment: PE-GNR + 7.5 W/cm^2 laser for 7 minutes.	30±0.3
e	Laser treatment: PE-GNR + 15 W/cm^2 laser for 7 minutes.	35±0.6
f	Laser treatment: PE-GNR + 20 W/cm^2 laser for 7 minutes.	41±1.0
g	Laser treatment: PE-GNR + 25 W/cm^2 laser for 7 minutes.	43±0.6

Figure 7. Photothermal ablation of PC3-PSMA human prostate cancer cells using EGDE-3,3′−PSS−CTAB−GNRs: (i) absorbance spectrum of EGDE-3,3′−PSS−CTAB−GNRs used in the photothermal ablation studies. (ii) Phase contrast images (A,C,E,G) and fluorescence microscopy images (B,D,F,H) of PC3-PSMA cells treated as described below; red fluorescence is due to ethidium homodimer staining of compromised nuclei. Scale bar: 200 μm. (A,B) EGDE-3,3′−PSS−CTAB−GNRs + laser (7 min; power density: 20 W/cm^2); (C,D) EGDE-3,3′−PSS−CTAB−GNRs (without laser treatment); (E,F) laser alone (no nanorods); (G,H) no treatment. (iii) Photothermal ablation of PC3-PSMA cells using EGDE-3,3′−PSS−CTAB−GNR (PE−GNR) assemblies (OD = 0.1) as a function of laser power density.

ability was determined 24 h after the photothermal treatment. It is possible that a significant number cells die due to the bystander effect[52] over the 24 h period following signals from those cells directly in the path of the laser. However, we have not directly determined the role of the bystander effect on PE−GNR induced hyperthermic ablation of cancer cells as part of this investigation. Nevertheless, these two factors can explain the high levels of PC3-PSMA cell death observed in these experiments. As may be expected, higher laser power densities resulted in higher (>85%) PC3-PSMA cell death. Cells treated with the laser alone (without PE−GNRs) and PE−GNRs alone (without laser irradiation) did not induce PC3-PSMA cell death.

While the above results are encouraging, it is important to point out that a balance exists between polyelectrolyte cytotoxicty and PE−GNR-induced hyperthermic ablation of cancer cells. While low concentrations of PE−GNRs are not sufficient for either stabilizing GNRs or for inducing hyperthermic temperatures, higher concentrations are cytotoxic and are therefore, not useful in hyperthermic ablation of cancer cells. As a result, we chose those concentrations of EGDE-3,3′−PSS−CTAB−GNRs that were not toxic to PC3-PSMA cells but demonstrated photothermal activity for the ablation of these cells. In contrast, pEI25-coated GNRs were highly toxic to the cells at concentrations that would result in hyperthermic temperatures (>40 °C) and therefore, were not included in this study. The use of such untargeted PE−GNRs can be useful in the hyperthermic ablation of relatively accessible tumors such as bladder or prostate tumors.

EGDE-3,3′−PSS−CTAB−GNRs Successfully Deliver Exogenous DNA to Prostate Cancer Cells *in Vitro*. Cationic polymers have emerged as promising candidates for delivering exogenous nucleic acids, including plasmid DNA, to a variety of mammalian cells. We asked whether stable PE−GNR assemblies could be employed to bind and deliver plasmid DNA to PC3-PSMA cells *in vitro*. Greater than 95% of the original plasmid DNA amount (350 ng) was loaded on PE−GNRs, while only 50−55% was loaded on equivalent amounts of CTAB−GNRs (Supporting Information, Table S1). Different subtoxic concentrations of PE−GNRs loaded with pGL3 plasmid DNA were delivered to PC3-PSMA cells. GNR concentrations were kept below OD = 0.25×10^{-2} in order to compare the transfection activity of EGDE-3,3′ polymer with that of pEI25 which was toxic to cells beyond this concentration (Figure 5). EGDE-3,3′-based PE−GNRs resulted in up to 10-fold higher gene expression in PC3-PSMA cells com-

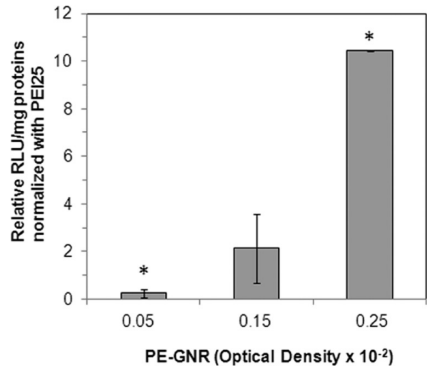

Figure 8. Transfection of PC3-PSMA human prostate cancer cells using EGDE-3,3′−PSS−CTAB−GNRs and pEI25-PSS−CTAB−GNRs. PC3-PSMA cells were treated with different concentrations of PE−GNRs containing 350 ng pGL3 plasmid for 6 h. Luciferase expression, in relative luminescence units or RLU was analyzed 48 h following transfection and normalized to protein content in each case (RLU /mg). The normalized luciferase expression for EGDE-3,3′−PSS−CTAB−GNRs is reported relative to that for pEI25-PSS−CTAB−GNRs. CTAB−GNRs did not demonstrate any transfection activity at similar optical densities. Asterisks (*) indicate *p* values < 0.02 determined using two-tailed Student's *t* test for a minimum of three independent experiments.

pared to pEI25-based PE−GNRs (Figure 8) after 48 h following transfection. CTAB−GNRs did not demonstrate any transfection activity under these conditions (not shown), presumably because of a combination of low DNA loading, nanoparticle aggregation which can lead to reduced cellular uptake, and inherently poor transfection efficacy.[53,54] The use of polyelectrolytes not only overcomes the poor GNR stability associated with CTAB, but also facilitates higher plasmid DNA binding and enhanced transfection activity of the resulting assemblies. The lower cytotoxicity of EGDE-3,3′−PSS−CTAB−GNRs makes it an attractive vector for nonviral gene delivery, compared to assemblies based on pEI25. Taken together, these results indicate that interfacing engineered polyelectrolytes with gold nanorods results in stable multifunctional assemblies that possess photothermal ablation, gene delivery, and optical imaging capabilities,[10,14,55−57] all on a single platform.

CONCLUSIONS

We have demonstrated that gold nanorods prepared using the CTAB-based seed-mediated method are poorly stable in phosphate buffered saline (PBS), serum-free media (SFM), and serum-containing media (SCM) following centrifugation. We employed the layer-by-layer deposition of polyelectrolytes in order to enhance the short-term and long-term stability of gold nanorods in these media. Polyelectrolyte-coated gold nanorods (PE−GNRs) demonstrate excellent long-term optical stability in all three media as determined by their optical properties even after 4 weeks of storage. Stabilization of the optical response, in turn, resulted in a reliable photothermal response of the well-dispersed gold nanorods over the period investigated, which facilitated their successful use in the photothermal ablation of PC3-PSMA human prostate cancer cells using near-infrared laser irradiation. Gold nanorods coated with the recently developed EGDE-3,3′ polymer in our laboratory demonstrated lower cytotoxicities and higher transfection efficacies than 25 kDa poly(ethylene imine), which is a current standard for polymer-mediated gene delivery. While EGDE-3,3′-coated GNRs demonstrated higher toxicities than CTAB−GNRs at similar optical densities, PE−GNRs possess greater advantages including stable photothermal properties, higher transfection efficacies, and the ability to further derivatize residual reactive amines.[51] These results indicate that molecular engineering of cationic polyelectrolytes can lead to stable, biocompatible, and multifunctional gold nanorod assemblies, which can be useful for a variety of simultaneous applications including optical imaging, nonviral gene delivery, and localized hyperthermia. Further discovery and engineering of polyelectrolytes that optimize toxicity, stability, and gene delivery efficacy will be required in case of polyelectrolyte-coated assemblies. While the current *in vitro* results are indeed encouraging, future studies on therapeutic efficacy, biocompatibility, and biodistribution in appropriate animal models will be needed in order to fully realize the potential of these assemblies.

EXPERIMENTAL SECTION

Materials. Sodium borohydride, powder, reagent grade, ≥98.5%, cetyltrimethylammonium bromide (CTAB), 95%, gold(III) chloride trihydrate ($HAuCl4 \cdot 3H_2O$), 99.9+%, L-ascorbic acid, reagent grade, ethyleneglycol diglycidyl ether (EDGE), 3,3′-diamino-*N*-methyl dipropylamine (3,3′), and branched poly(ethyleneimine) ($M_W = 25000$, $M_N = 10000$; henceforth called pEI25) were purchased from Sigma-Aldrich. Crystalline silver nitrate was purchased from Spectrum and poly(styrene sulfonate) (sodium salt; henceforth called PSS) ($M_W = 14900$) was purchased from Polysciences, Inc. All materials were used as received without further purification.

Generation of Gold Nanorods. Gold nanorods were synthesized using the seed-mediated method as described by El-Sayed *et al.*[35] Briefly, a seed solution was prepared by adding 0.6 mL of iced water-cooled sodium borohydride (0.01 M) in order to reduce a solution of 5 mL of CTAB (0.2 M) (cetyltrimethylammonium bromide) in 5 mL of auric acid (0.0005 M) ($HAuCl_4 \cdot 3H_2O$). The growth solution was prepared by reducing 5 mL of CTAB (0.2 M) in 5 mL of auric acid (0.001M) ($HAuCl_4 \cdot 3H_2O$) containing 250 μL of silver nitrate (0.004 M) with 70 μL of L-ascorbic acid (0.0788 M) solution. Seed solution (12 μL) was added to a 10 mL growth solution which resulted in the generation of gold nanorods after 4 h of continuous stirring. Gold nanorods that possessed absorbance maxima (λ_{max}) at different wavelengths (750−900 nm) in the near-infrared (NIR) region of the absorption spectrum were generated by slightly increasing or decreasing silver nitrate amount in this method.

Polymer Synthesis and Characterization. Polymerizations were carried out as described previously.[51] Briefly, ethyleneglycol digly-

TABLE 1. Composition of the PE−GNR Assemblies Employed in the Current Investigation

first layer polyelectrolyte	polyelectrolyte concentration (mg/mL)	second layer polyelectrolyte	polyelectrolyte concentration (mg/mL)					
PSS	2	EGDE-3,3′	0	0.2	0.4	1	2	3
PSS	2	25 kDa pEI	0.2	0.4	1	2	3	4

cidylether (EGDE; 2.3 mmol) was reacted with equimolar quantities of 3,3′-diamino-*N*-methyl dipropylamine (3,3′) resulting in the formation of the EGDE-3,3′ cationic polymer. Neat, as-purchased solutions were employed in the polymerization reaction, which was carried out in 7 mL glass scintillation vials for 16 h. Following completion of the reaction, the resulting polymer was diluted to a concentration of 2 mg/mL in phosphate-buffered saline (0.01 X PBS). The solution pH was adjusted to 7.4 using 30% hydrochloric acid in deionized (DI) water in order to compensate for the basicity of the cationic polymer. Polymer formation was confirmed using Fourier transform infrared (FT-IR) spectroscopy, and the molecular weight was determined using gel-permeation chromatography as described previously.[51]

Generation of Polyelectrolyte (PE)−Gold Nanorod (PE−GNR) Dispersions. Gold nanorods were modified with polyelectrolytes (PEs) using a layer-by-layer deposition approach. Briefly, gold nanorods (optical density 0.5), in 1.5 mL microcentrifuge tubes, were first centrifuged at 6000 rcf for 10 min using a Microfuge 18 centrifuge (Beckman Coulter) in order to remove excess CTAB. Following removal of the supernatant, nanorods were resuspended in 0.5 mL of poly(styrene sulfonate) or PSS solution (2 mg/mL PSS in 0.01X PBS; ~1.5 mM salt concentration) and were immediately sonicated for 25 min leading to the formation of PSS−CTAB−GNRs. Excess PSS was removed by centrifugation at 6000 rcf for 10 min, and different amounts of cationic polyelectrolytes, either pEI25 or EGDE-3,3′ polymer, were added and sonicated for 25 min leading to the formation of pEI25−PSS−CTAB−GNRs or EGDE-3,3′−PSS−CTAB−GNRs. Finally, cationic polyelectrolyte coated gold nanorods (PE−GNRs) were centrifuged and resuspended in different aqueous media (DI water, PBS, serum-free media, or serum-containing media) to monitor their stability. The conditions for generating these different PE−GNRs are summarized in Table 1.

Determination of Short- and Long-Term Optical Stability. CTAB−gold nanorods with optical density 0.5 at 800 nm were first prepared and dispersed in DI water using the seed-mediated method. Aliquots (0.5 mL) of CTAB gold nanorods, placed in 1.5 mL centrifuge tubes, were centrifuged and resuspended in the same volume of DI water, 1X PBS, serum-free medium (SFM) or serum-containing medium (SCM). Absorption spectra were determined at different times using a temperature-controlled plate reader (Biotek Synergy 2) for up to 48 h; spectra were typically measured between 400−999 nm. Absorbance spectra were monitored every week for a period of 4 weeks as described above for long -term optical stability studies.

Determination of Photothermal Response.[19] Dispersions of CTAB- (1 h) or PE-coated (1 h and 4 weeks) gold nanorods in serum free media (RPMI-1640 medium plus 1% penicillin/streptomycin) were employed for determining the temperature response of gold nanorods following exposure to near-infrared (NIR) laser treatment. Stable, EGDE-3,3′−PSS−CTAB−gold nanorods were prepared and diluted to form a stock solution with a maximum optical density of 0.22 at 770 nm (maximal absorbance wavelength). A titanium CW sapphire (Ti:S) laser (Spectra-Physics, Tsunami) pumped by a solid state laser (Spectra-Physics, Millennia) was used for determining the photothermal response. Samples were diluted and placed in a 96-well plate (diameter ~6.4 mm, height ~10.7 mm) in the path of the laser (diameter of the laser spot was 2 mm). The laser was turned on for 15 min and the temperature of the dispersion was monitored using a K-type thermocouple; laser output was fixed at 600 mW (20 W/cm^2).

Cell Culture. The PC3-PSMA human prostate cancer cell line[58] was a generous gift from Dr. Michel Sadelain of the Memorial Sloan Cancer Center, New York, NY. RPMI 1640 with L-glutamine and HEPES (RPMI-1640 medium), Pen-Strep solution: 10000 units/mL penicillin and 10000 μg/mL streptomycin in 0.85% NaCl, and fetal bovine serum (FBS) were purchased from Hyclone. Serum-free medium (SFM) is RPMI-1640 medium plus 1% antibiotics. Serum-containing medium is SFM plus 10% FBS. Cells were cultured in a 5% CO_2 incubator at 37 °C using RPMI-1640 medium containing 10% heat-inactivated fetal bovine serum (FBS) and 1% antibiotics (10000 units/mL penicillin G and 10000 μg/mL streptomycin).

Cytotoxicity of Polyelectrolyte (PE)-Coated Gold Nanorods. Stable polyelectrolyte (EGDE-3,3′−PSS−CTAB and pEI25−PSS−CTAB) gold nanorods with an absorbance maximum at 770 nm were prepared as described above. PC3-PSMA human prostate cancer cells were seeded in a 24-well plate with a density of 50000 cells/well and allowed to attach overnight at 37 °C, in a 5% CO_2 incubator. Different amounts of polyelectrolyte-coated gold nanorods (PE−GNRs, dispersed in serum-free media) were added into each well, and the final volume in each well was brought up to 500 μL with serum-free media. Cells were incubated for 5 h to determine the cytotoxicity of PE−GNR assemblies. Following incubation, cells were treated with 100 μL of 4 μM ethidium homodimer-1 (EthD-1; Invitrogen) and 2 μM calcien AM (Invitrogen) for 30 min and imaged immediately using Zeiss AxioObserver D1 inverted microscope (10 × X/0.3 numerical aperture (NA) objective; Carl Zeiss MicroImaging Inc., Germany). Fluorescence using excitation at 530 nm and emission at 645 nm were used for the microscopy; dead/dying cells with compromised nuclei stained positive (red) for EthD-1. Quantitative analysis of PE−GNR-induced cell death was carried out by manually counting the number of dead cells in all cases using the Cell Counter plug-in in ImageJ software (Rasband, W. S., ImageJ, U.S. National Institutes of Health, Bethesda, MD, http://rsb.info.nih.gov/ij/, 1997−2005). The number of dead cells in both live and dead controls was determined for at least two independent experiments, and their average values were calculated. The number and percentage of red fluorescent cells was determined for each concentration of PE−GNR assemblies as a function of dose.

Photothermal Ablation of PC3-PSMA Cells Using EGDE-3,3′−PSS−CTAB−GNRs. Stable polyelectrolyte gold nanorods (EGDE-3,3′−PSS−CTAB−GNR) with an optical density 0.2 at 800 nm were prepared as described above. PC3-PSMA human prostate cancer cells were seeded in a 96-well plate with a density of 30000 cells/well and allowed to attach overnight at 37 °C, in a 5% CO_2 incubator. PE−GNRs (EGDE-3,3′−PSS−CTAB−GNR) were diluted to an optical density of 0.1 with serum-free media. The laser excitation source was tuned to 800 nm in order to coincide with the longitudinal absorption maximum of the EGDE-3,3′−PSS−CTAB−GNR. First, cell culture media was replaced by 200 μL of EGDE-3,3′−PSS−CTAB−GNR solution (optical density 0.1) followed by exposure to laser irradiation for 7 min at different power densities (7.5−25 W/cm^2). The temperature of the dispersion was measured using a K-type thermocouple immediately after removal of the laser treatment. Following treatment, EGDE-3,3′−PSS−CTAB−GNR containing media was removed and immediately replaced with fresh serum-containing cell culture media and the cells were returned to the 37 °C incubator. After 24 h, cells were treated with 4 μM ethidium homodimer-1 (EthD-1; Invitrogen) for 30 min and imaged using Zeiss AxioObserver D1 inverted microscope (10 × X/0.3 numerical aperture (NA) objective; Carl Zeiss MicroImaging Inc., Germany). Fluorescence using excitation at 530 nm and emission at 645 nm were used for the microscopy; dead/dying cells with compromised nuclei stained positive (red) for EthD-1. Quantitative analysis of PE−GNR induced cell death was carried out by manually counting the number of dead cells in all cases using the Cell Counter plug-in in ImageJ software (Rasband, W. S., ImageJ, U.S. National Institutes of Health, Bethesda, MD, http://rsb.info.nih.gov/ij/, 1997−2005). The number of dead cells in both live and dead controls was determined for at least two independent experiments, and their average values were calculated.

Transfection of PC3-PSMA Cells Using PE−GNRs. *Plasmid DNA.* The pGL3 control vector (Promega Corp., Madison, WI), which encodes for the modified firefly luciferase protein under the control of an SV40 promoter, was used in transfection experiments. E.coli (XL1 Blue) cells containing the pGL3 plasmid DNA were cultured overnight (16 h, 37 °C, 150 rpm) in 15 mL tubes

(Fisher) in 5 mL of Terrific Broth (MP Biomedicals, LLC) containing 1 mg/mL ampicillin (Research Products International, Corp.). The cultures were then centrifuged at 5400*g* and 4 °C for 10 min. Plasmid DNA was purified according to the QIAprep Miniprep Kit (Qiagen) protocol and DNA concentration and purity were determined based on absorbance at 260 and 280 nm determined using NanoDrop spectrophotometer (ND-1000; NanoDrop Technologies). Plasmid DNA concentrations of 100−130 ng/μL were used in all experiments and the volume was adjusted in order to load 350 ng of plasmid amounts (ng) on PE−GNRs prior to transfection.

DNA Loading on PE−GNRs. PE−GNRs (optical density 0.25×10^{-2}) were mixed with 350 ng of pGL3 plasmid DNA in the presence of serum-free media for 30 min. The PE−GNR−pGL3 plasmid assemblies were then centrifuged at 6000 rcf for 10 min. The plasmid amount of DNA remaining in the supernatant after centrifugation was determined using calibration of fluorescence intensity *vs* plasmid DNA concentration (not shown); ethidium bromide was used for calibrating DNA amounts.

Transfections. PC3-PSMA cells were cultured as described above. Cells were seeded in 24-well plates (Costar) at a density of 50000 cells/well and allowed to attach overnight. PE−GNR−pGL3 plasmid assemblies were added to each well in the presence of serum-free media for 6 h; CTAB−GNRs with equivalent amounts of plasmid DNA were used as controls. The media was then replaced with serum-containing media for 48 h following which cells were permeabilized with 100 μL of cell lysis buffer (Promega, Madison, WI). The luciferase activity in cell lysates was measured using a luciferase assay kit (Promega, Madison, WI) using a plate reader (Bio-Tek Synergy 2). The relative light units (RLU) determined from the assay were normalized with respect to protein concentration in the cell lysates, measured using the Pierce BCA Protein Assay Kit (Pierce Biotechnology, Rockford, IL). Luciferase activity in cell lysates was expressed as relative light units (RLU) per milligram (mg) of protein. Transfection experiments were performed at least in triplicate.

Acknowledgment. The authors thank Dr. Su Lin and Professor Neal Woodbury, Director, Center for Bio-Optical Nanotechnology at The Biodesign Institute, ASU for access to the laser facility. The authors also thank Mr. Fred Penã at ASU for invaluable technical assistance. This work was supported by and National Science Foundation Grant CBET-0829128, National Institutes of Health Grant 5R21CA133618-02, and start-up funds from the state of Arizona to K.R., and by the Fulton Undergraduate Research Initiative (FURI) Award at ASU to D.B.K.

Note added after print publication: Production error caused two panels of Figure 7 to be cut off in the issue publication October 2009.

Supporting Information Available: Plasmid DNA loading on CTAB−GNRs, EGDE-3,3′−PSS−TAB−GNRs, and pEI25k−PSS−CTAB−GNRs. This material is available free of charge *via* the Internet at http://pubs.acs.org.

REFERENCES AND NOTES

1. Jabr-Milane, L.; van Vlerken, L.; Devalapally, H.; Shenoy, D.; Komareddy, S.; Bhavsar, M.; Amiji, M. Multifunctional Nanocarriers for Targeted Delivery of Drugs and Genes. *J. Controlled Release* **2008**, *130*, 121–128.
2. Smith, A. M.; Duan, H.; Mohs, A. M.; Nie, S. Bioconjugated Quantum Dots for *in Vivo* Molecular and Cellular Imaging. *Adv. Drug Delivery Rev.* **2008**, *60*, 1226–1240.
3. Cho, K.; Wang, X.; Nie, S.; Chen, Z. G.; Shin, D. M. Therapeutic Nanoparticles for Drug Delivery in Cancer. *Clin. Cancer Res.* **2008**, *14*, 1310–1316.
4. Medintz, I. L.; Mattoussi, H.; Clapp, A. R. Potential Clinical Applications of Quantum Dots. *Int. J. Nanomed.* **2008**, *3*, 151–167.
5. Heath, J. R.; Davis, M. E. Nanotechnology and Cancer. *Annu. Rev. Med.* **2008**, *59*, 251–265.
6. Lee, K. S.; El-Sayed, M. A. Gold and Silver Nanoparticles in Sensing and Imaging: Sensitivity of Plasmon Response to Size, Shape, and Metal Composition. *J. Phys. Chem.* **2006**, *110*, 19220–19225.
7. Lee, K. S.; El-Sayed, M. A. Dependence of the Enhanced Optical Scattering Efficiency Relative to That of Absorption for Gold Metal Nanorods on Aspect Ratio, Size, End-Cap Shape, and Medium Refractive Index. *J. Phys. Chem. B* **2005**, *109*, 20331–20338.
8. El-Sayed, I. H.; Huang, X.; El-Sayed, M. A. Surface Plasmon Resonance Scattering and Absorption of anti-EGFR Antibody Conjugated Gold Nanoparticles in Cancer Diagnostics: Applications in Oral Cancer. *Nano Lett.* **2005**, *5*, 829–834.
9. Huang, X.; El-Sayed, I. H.; Qian, W.; El-Sayed, M. A. Cancer Cells Assemble and Align Gold Nanorods Conjugated to Antibodies to Produce Highly Enhanced, Sharp, and Polarized Surface Raman Spectra: A Potential Cancer Diagnostic Marker. *Nano Lett.* **2007**, *7*, 1591–1597.
10. Huang, X.; El-Sayed, I. H.; Qian, W.; El-Sayed, M. A. Cancer Cell Imaging and Photothermal Therapy in the Near-Infrared Region by Using Gold Nanorods. *J. Am. Chem. Soc.* **2006**, *128*, 2115–2120.
11. Huang, Y. F.; Chang, H. T.; Tan, W. Cancer Cell Targeting Using Multiple Aptamers Conjugated on Nanorods. *Anal. Chem.* **2008**, *80*, 567–572.
12. Skirtach, A. G.; Dejugnat, C.; Braun, D.; Susha, A. S.; Rogach, A. L.; Parak, W. J.; Mohwald, H.; Sukhorukov, G. B. The Role of Metal Nanoparticles in Remote Release of Encapsulated Materials. *Nano Lett.* **2005**, *5*, 1371–1377.
13. Salem, A. K.; Searson, P. C.; Leong, K. W. Multifunctional Nanorods for Gene Delivery. *Nat. Mater.* **2003**, *2*, 668–671.
14. Durr, N. J.; Larson, T.; Smith, D. K.; Korgel, B. A.; Sokolov, K.; Ben-Yakar, A. Two-Photon Luminescence Imaging of Cancer Cells Using Molecularly Targeted Gold Nanorods. *Nano Lett.* **2007**, *7*, 941–945.
15. Sonnichsen, C.; Alivisatos, A. P. Gold Nanorods as Novel Nonbleaching Plasmon-Based Orientation Sensors for Polarized Single-Particle Microscopy. *Nano Lett.* **2005**, *5*, 301–304.
16. Yu, C.; Irudayaraj, J. Multiplex Biosensor Using Gold Nanorods. *Anal. Chem.* **2007**, *79*, 572–579.
17. York, J.; Spetzler, D.; Xiong, F.; Frasch, W. D. Single-Molecule Detection of DNA *via* Sequence-Specific Links between F1-ATPase Motors and Gold Nanorod Sensors. *Lab Chip* **2008**, *8*, 415–419.
18. Sun, Z.; Ni, W.; Yang, Z.; Kou, X.; Li, L.; Wang, J. pH-Controlled Reversible Assembly and Disassembly of Gold Nanorods. *Small* **2008**, *4*, 1287–1292.
19. Huang, H. C.; Koria, P.; Parker, S. M.; Selby, L.; Megeed, Z.; Rege, K. Optically Responsive Gold Nanorod-Polypeptide Assemblies. *Langmuir* **2008**, *24*, 14139–14144.
20. Huang, X.; Jain, P. K.; El-Sayed, I. H.; El-Sayed, M. A. Gold Nanoparticles: Interesting Optical Properties and Recent Applications in Cancer Diagnostics and Therapy. *Nanomedicine* **2007**, *2*, 681–693.
21. Skrabalak, S. E.; Chen, J.; Au, L.; Lu, X.; Li, X.; Xia, Y. Gold Nanocages for Biomedical Applications. *Adv. Mater.* **2007**, *19*, 3177–3184.
22. Dickerson, E. B.; Dreaden, E. C.; Huang, X.; El-Sayed, I. H.; Chu, H.; Pushpanketh, S.; McDonald, J. F.; El-Sayed, M. A. Gold nanorod Assisted near-Infrared Plasmonic Photothermal Therapy (PPTT) of Squamous Cell Carcinoma in Mice. *Cancer Lett.* **2008**, *269*, 57–66.
23. Hosta, L.; Pla-Roca, M.; Arbiol, J.; Lopez-Iglesias, C.; Samitier, J.; Cruz, L. J.; Kogan, M. J.; Albericio, F. Conjugation of Kahalalide F with Gold Nanoparticles to Enhance *in Vitro* Antitumoral Activity. *Bioconjugate Chem.* **2009**, *20*, 138–146.
24. Oo, M. K.; Yang, X.; Du, H.; Wang, H. 5-Aminolevulinic Acid-Conjugated Gold Nanoparticles for Photodynamic Therapy of Cancer. *Nanomedicine* **2008**, *3*, 777–786.
25. Dhar, S.; Reddy, E. M.; Shiras, A.; Pokharkar, V.; Prasad, B. L. Natural Gum Reduced/Stabilized Gold Nanoparticles for Drug Delivery Formulations. *Chemistry* **2008**, *14*, 10244–10250.

26. Ghosh, P.; Han, G.; De, M.; Kim, C. K.; Rotello, V. M. Gold Nanoparticles in Delivery Applications. *Adv. Drug Delivery Rev.* **2008**, *60*, 1307–1315.
27. Shi, X.; Wang, S.; Meshinchi, S.; Van Antwerp, M. E.; Bi, X.; Lee, I.; Baker, J. R., Jr. Dendrimer-Entrapped Gold Nanoparticles As a Platform for Cancer-Cell Targeting and Imaging. *Small* **2007**, *3*, 1245–1252.
28. Joshi, H. M.; Bhumkar, D. R.; Joshi, K.; Pokharkar, V.; Sastry, M. Gold Nanoparticles As Carriers for Efficient Transmucosal Insulin Delivery. *Langmuir* **2006**, *22*, 300–305.
29. Lee, S. H.; Bae, K. H.; Kim, S. H.; Lee, K. R.; Park, T. G. Amine-Functionalized Gold Nanoparticles As Non-Cytotoxic and Efficient Intracellular siRNA Delivery Carriers. *Int. J. Pharm.* **2008**, *364*, 94–101.
30. Ghosh, P. S.; Kim, C. K.; Han, G.; Forbes, N. S.; Rotello, V. M. Efficient Gene Delivery Vectors by Tuning the Surface Charge Density of Amino Acid-Functionalized Gold Nanoparticles. *ACS Nano* **2008**, *2*, 2213–2218.
31. Rhim, W. K.; Kim, J. S.; Nam, J. M. Lipid−Gold-Nanoparticle Hybrid-Based Gene Delivery. *Small* **2008**, *4*, 1651–1655.
32. Thomas, M.; Klibanov, A. M. Conjugation to Gold Nanoparticles Enhances Polyethylenimine'S Transfer of Plasmid DNA into Mammalian Cells. *Proc. Natl. Acad. Sci. U.S.A.* **2003**, *100*, 9138–9143.
33. Sandhu, K. K.; McIntosh, C. M.; Simard, J. M.; Smith, S. W.; Rotello, V. M. Gold Nanoparticle-Mediated Transfection of Mammalian Cells. *Bioconjugate Chem.* **2002**, *13*, 3–6.
34. Ow Sullivan, M. M.; Green, J. J.; Przybycien, T. M. Development of a Novel Gene Delivery Scaffold Utilizing Colloidal Gold-Polyethylenimine Conjugates for DNA Condensation. *Gene Ther.* **2003**, *10*, 1882–1890.
35. Nikoobakht, B.; El-Sayed, M. A. Preparation and Growth Mechanism of Gold Nanorods (NRs) Using Seed-Mediated Growth Method. *Chem. Mater.* **2003**, *15*, 1957–1962.
36. van der Zande, B. M. I.; Bohmer, M. R.; Fokkink, L. G. J.; Schonenberger, C. Colloidal Dispersions of Gold Rods: Synthesis and Optical Properties. *Langmuir* **2000**, *16*, 451–458.
37. Burdick, J.; Alonas, E.; Huang, H. C.; Rege, K.; Wang, J. High-Throughput Templated Multisegment Synthesis of Gold Nanowires and Nanorods. *Nanotechnology* **2009**, *20*, 65306.
38. Takahashi, H.; Niidome, Y.; Niidome, T.; Kaneko, K.; Kawasaki, H.; Yamada, S. Modification of Gold Nanorods Using Phosphatidylcholine to Reduce Cytotoxicity. *Langmuir* **2006**, *22*, 2–5.
39. Goodwin, A. P.; Tabakman, S. M.; Welsher, K.; Sherlock, S. P.; Prencipe, G.; Dai, H. Phospholipid-Dextran with a Single Coupling Point: A Useful Amphiphile for Functionalization of Nanomaterials. *J. Am. Chem. Soc.* **2009**, *131*, 289–296.
40. Wijaya, A.; Hamad-Schifferli, K. Ligand Customization and DNA Functionalization of Gold Nanorods *via* Round-Trip Phase Transfer Ligand Exchange. *Langmuir* **2008**, *24*, 9966–9969.
41. Niidome, T.; Yamagata, M.; Okamoto, Y.; Akiyama, Y.; Takahashi, H.; Kawano, T.; Katayama, Y.; Niidome, Y. PEG-Modified Gold Nanorods with a Stealth Character for *in Vivo* Applications. *J. Controlled Release* **2006**, *114*, 343–347.
42. Choi, B. S.; Iqbal, M.; Lee, T.; Kim, Y. H.; Tae, G. Removal of Cetyltrimethylammonium Bromide to Enhance the Biocompatibility of Au Nanorods Synthesized by a Modified Seed Mediated Growth Process. *J. Nanosci. Nanotechnol.* **2008**, *8*, 4670–4674.
43. Gole, A.; Murphy, C. J. Polyelectrolyte-Coated Gold Nanorods: Synthesis, Characterization and Immobilization. *Chem. Mater.* **2005**, *17*, 1325–1330.
44. Ding, H.; Yong, K.-T.; Roy, I.; Pudavar, H. E.; Law, W. C.; Bergey, E. J.; Prasad, P. N. Gold Nanorods Coated with Multilayer Polyelectrolyte as Contrast Agents for Multimodal Imaging. *J. Phys. Chem. C* **2007**, *111*, 12552–12557.
45. Connor, E. E.; Mwamuka, J.; Gole, A.; Murphy, C. J.; Wyatt, M. D. Gold Nanoparticles Are Taken up by Human Cells but Do Not Cause Acute Cytotoxicity. *Small* **2005**, *1*, 325–327.
46. Srivastava, S.; Kotov, N. A. Composite Layer-by-Layer (LBL) Assembly with Inorganic Nanoparticles and Nanowires. *Acc. Chem. Res.* **2008**, *41*, 1831–1841.
47. Chithrani, B. D.; Ghazani, A. A.; Chan, W. C. Determining the Size and Shape Dependence of Gold Nanoparticle Uptake into Mammalian Cells. *Nano Lett.* **2006**, *6*, 662–668.
48. Kaufman, E. D.; Belyea, J.; Johnson, M. C.; Nicholson, Z. M.; Ricks, J. L.; Shah, P. K.; Bayless, M.; Pettersson, T.; Feldoto, Z.; Blomberg, E.; Claesson, P.; Franzen, S. Probing Protein Adsorption onto Mercaptoundecanoic Acid Stabilized Gold Nanoparticles and Surfaces by Quartz Crystal Microbalance and Zeta-Potential Measurements. *Langmuir* **2007**, *23*, 6053–6062.
49. Huang, X. H.; El-Sayed, I. H.; Qian, W.; El-Sayed, M. A. Cancer Cell Imaging and Photothermal Therapy in the Near-Infrared Region by Using Gold Nanorods. *J. Am. Chem. Soc.* **2006**, *128*, 2115–2120.
50. Huff, T. B.; Hansen, M. N.; Zhao, Y.; Cheng, J. X.; Wei, A. Controlling the Cellular Uptake of Gold Nanorods. *Langmuir* **2007**, *23*, 1596–1599.
51. Barua, S.; Joshi, A.; Banerjee, A.; Matthews, D.; Sharfstein, S. T.; Cramer, S. M.; Kane, R. S.; Rege, K. Parallel Synthesis and Screening of Polymers for Nonviral Gene Delivery. *Mol. Pharm.* **2009**, *6*, 86–97.
52. Everts, M.; Saini, V.; Leddon, J. L.; Kok, R. J.; Stoff-Khalili, M.; Preuss, M. A.; Millican, C. L.; Perkins, G.; Brown, J. M.; Bagaria, H.; Nikles, D. E.; Johnson, D. T.; Zharov, V. P.; Curiel, D. T. Covalently Linked Au Nanoparticles to a Viral Vector: Potential for Combined Photothermal and Gene Cancer Therapy. *Nano Lett.* **2006**, *6*, 587–591.
53. Tang, F.; Hughes, J. A. Synthesis of a Single-Tailed Cationic Lipid and Investigation of Its Transfection. *J. Controlled Release* **1999**, *62*, 345–358.
54. Yu, W.; Liu, C.; Ye, J.; Zou, W.; Zhang, N.; Xu, W. Novel Cationic SLN Containing a Synthesized Single-Tailed Lipid As a Modifier for Gene Delivery. *Nanotechnology* **2009**, *20*, 215102.
55. Tong, L.; Wei, Q.; Wei, A.; Cheng, J. X. Gold Nanorods As Contrast Agents for Biological Imaging: Optical Properties, Surface Conjugation and Photothermal Effects. *Photochem. Photobiol.* **2009**, *85*, 21–32.
56. Park, J.; Estrada, A.; Sharp, K.; Sang, K.; Schwartz, J. A.; Smith, D. K.; Coleman, C.; Payne, J. D.; Korgel, B. A.; Dunn, A. K.; Tunnell, J. W. Two-Photon-Induced Photo-luminescence Imaging of Tumors Using Near-Infrared Excited Gold Nanoshells. *Opt. Express* **2008**, *16*, 1590–1599.
57. Eghtedari, M.; Oraevsky, A.; Copland, J. A.; Kotov, N. A.; Conjusteau, A.; Motamedi, M. High Sensitivity of *in Vivo* Detection of Gold Nanorods Using a Laser Optoacoustic Imaging System. *Nano Lett.* **2007**, *7*, 1914–1918.
58. Gong, M. C.; Latouche, J. B.; Krause, A.; Heston, W. D.; Bander, N. H.; Sadelain, M. Cancer Patient T Cells Genetically Targeted to Prostate-Specific Membrane Antigen Specifically Lyse Prostate Cancer Cells and Release Cytokines in Response to Prostate-Specific Membrane Antigen. *Neoplasia* **1999**, *1*, 123–127.